Int. J. Electrochem. Sci., 12 **(2017)** 10773 – 10782, doi: 10.20964/2017.11.36

International Journal of
ELECTROCHEMICAL
SCIENCE
www.electrochemsci.org

Electrochemical Determination of the Anticancer Drug Capecitabine Based on a Graphene-Gold Nanocomposite-Modified Glassy Carbon Electrode

Qibing Zhang[#], *Xiaojun Shan*[#], *Yu Fu, Pengyu Liu, Xiaofeng Li, Baocui Liu, Lijun Zhang and Dong Li*[*]

Department of General Surgery, Daqing Oilfield General Hospital, Daqing City, Heilongjiang Province, 163000, P.R. China
[#] These authors contributed equally to this work.
[*]E-mail: dongli_daqing@foxmail.com

Received: 31 July 2017 / *Accepted:* 5 September 2017 / *Published:* 12 October 2017

This study used a glassy carbon electrode (GCE) modified by gold nanoparticles (AuNPs) and stacked graphene nanofibres (SGNF) to prepare a facile electrochemical sensor for the detection of capecitabine, an anti-cancer drug used in breast cancer treatment. Differential pulse voltammetry (DPV) measurements were performed to investigate the electrochemical reduction of capecitabine using the AuNPs/SGNF-modified GCE. Our proposed sensor showed exceptional electrochemical activity to the capecitabine reduction with a linear range of 0.05 μM to 80.00 μM and a limit of detection (LOD) of 0.017 μM (S/N=3). Due to the distinct analysis behaviour, our proposed sensor shows potential for the practical detection of capecitabine in serum specimens.

Keywords: Capecitabine; Gold nanoparticles; Stacked graphene nanofibres; Electrochemical determination; Breast cancer

1. INTRODUCTION

As the most common cancer for women, breast cancer is the second leading cause of cancer-related deaths, with 212,930 new cases and 40,870 cancer-related deaths in 2005 [1]. Five-year survival rates decrease with advancing disease stage: from 98% in localized disease to 80% with regional spreading to only 26% with metastatic disease. In neoadjuvant, adjuvant, and metastatic settings, chemotherapy is a significant treatment of breast cancer. Single chemotherapeutic agents, i.e., capecitabine, vinorelbine, taxanes, and anthracyclines, are on the National Comprehensive Cancer Network (NCCN) listing of preferred single agents, and each of them may be used as a single agent for

recurrent or metastatic disease [2]. In particular, single-agent paclitaxel, a type of taxane, has been shown to be active as a first-line treatment for patients with metastatic disease, with recorded response rates in the range of 25% to 34% [3-6], and docetaxel has been shown to be active in previously treated metastatic settings, yielding response rates in the range of 33% to 43% [7-9]. It has been proved that 5-fluorouracil (5-FU) bolus infusions with leucovorin are substantively active, with response rates of 17% to 23% in patients with prior chemotherapy and 36% in chemotherapy-naïve patients [10-12]. The response rates of continuous infusion 5-FU with leucovorin was approximately 29% [13]. Nevertheless, continuous infusion treatment for breast cancer is inconvenient in terms of the cost of medical resources and the quality of life of the patients.

Capecitabine is a novel, orally administered fluoropyrimidine carbamate used to treat breast and colorectal cancers. Capecitabine can be easily absorbed by the gastrointestinal tract and metabolized by the enzyme carboxylesterase in the liver, where capecitabine is converted into 5′ deoxy-5-fluorocytidine (5′ DFCR) and further into 5′ deoxy-5-fluorouridine (5′ DFUR) (by cytidine deaminase) [14, 15]. 5′ DFUR is converted into 5-FU by thymidine phosphorylase (TP) in normal and tumour tissues. Unlike the parenterally administered 5-FU, orally administered capecitabine is predominantly found in tumour tissue instead of in adjacent healthy tissue and plasma [16]. Therefore, physicians treating breast cancer can mimic the effect of continuous infusion 5-FU with orally administered capecitabine in a convenient outpatient setting without the complications and costs related to infusion pumps and parenteral therapies [17]. Analytical strategies such as LC–MS, HPLC, and LC–MS/MS have been rarely proposed for the measurement of CPT in biological specimens [18-22]. These strategies are time consuming and require complex extraction and purification steps or on-line specimen extraction. Furthermore, the formulized measurement of CPT was not involved in these strategies. Additionally, considering the high cost of LC–MS/MS and LC-MS, the development of a novel analytical technique for the detection of CPT in its formulations is urgently needed.

Recently, electrochemical strategies have been well developed owing to their low cost, high sensitivity and short analysis time. Electroanalytical strategies could be further applied to the detection of reaction mechanisms. As a two-dimensional model for carbon-based electronic materials, graphene sheet has gained substantial attention recently. Owing to its distinct nanostructure and features, graphene has been considered a potential material for device applications as a desirable nanoscale building block. Stacked graphene nanofibres (SGNFs) involve layered graphene stacks containing many open graphene edges on their surfaces. This material has been considered to show potential for use in electrochemical sensors, owing to its distinct physico-chemical features such as high chemical stability, high elasticity, desirable catalytic properties, large specific surface area, and curved configuration [23-26]. Au nanoparticles (AuNPs) possess a desirable catalytic capability and high effective surface area, thus contributing to the enhancement of charge transfer and then electrode conductivity; these materials have therefore attracted substantial attention for use in biosensors, catalysis, and electronics. Based on previous reports in the literature, AuNP-modified electrodes have exhibited distinct electrocatalytic activity for a large number of biomolecules [27-30].

This study proposed the fabrication of a sensitive, facile, rapid and convenient electrochemical sensor based on the glassy carbon electrode (GCE) modified by AuNPs and SGNF nanocomposite for the detection of capecitabine. The nanocomposite was successfully used for the electrochemical

reduction of capecitabine at lower overpotentials as a distinct catalyst. The combination of SGNF and AuNPs contributed to high conductivity, large specific surface area, and considerable enhancement of electrocatalytic behaviour. This study also assessed the analytical behaviour of our developed system, and the parameters were optimized for the capecitabine detection in the biological matrix.

2. EXPERIMENTS

2.1. Chemicals

Stacked graphene nanofibres were commercially available from STREM Chemicals (Newburyport, MA, USA). Chloroauric acid was commercially available from Sigma–Aldrich (USA). Capecitabine was obtained from the Merck Company. For the preparation of the supporting electrolyte, i.e., phosphate buffer solution (PBS; 0.1 M), the stock solutions of Na_2HPO_4 (0.1 M) and NaH_2PO_4 (0.1 M) were mixed together, with further adjustment of the pH using NaOH or H_3PO_4 (0.1 M for each). Other reagents were of analytical chemical grade and were used as received. Doubly distilled water was used in all experiments.

2.2. Apparatus and characterizations

Electrochemical measurements were carried out using a CHI 832 electrochemical workstation (CHI Instruments, Chenhua, Shanghai, China) equipped with a traditional three-electrode geometry, where the working, reference and counter electrodes were a bare glass carbon electrode (GCE) or modified GCE, a saturated calomel electrode (SCE), and a platinum sheet, respectively. The electrochemical impedance spectroscopy (EIS) experiments were carried out using VMP2 multi-channel potentiostats. A multi-impedance test configuration was used for the electrochemical impedance spectroscopy analysis, for which the AC amplitude was 10 mV and the frequency ranged from 10 kHz to 10 mHz. CV was performed at the scan rate of 100 mV/s, and the potential range was 0.0-1.0 V. DPV measurements were also carried out, for which the step potential and pulse amplitude were 2 mV and 25 mV, respectively. We also applied a 20 ms pulse, a scan rate of 10 mV/s, and a sampling time of 20 ms, along with a 100 ms pulse interval.

2.3. Electrode preparation

Prior to use, GCEs with a diameter of 3 mm were polished to a mirror-like finish using alumina slurries (0.3 and 0.05 μm) sequentially on a polishing cloth with complete rinsing using doubly distilled water conducted between polishing steps. This was followed by sonication using ethanol and doubly distilled water and then air drying. The AuNPs/SGNF/GCE was prepared as follows. First, SGNF (10 mg) was dispersed in doubly distilled water (10 mL), and a homogenous dispersion was obtained after 60 min of sonication. This was followed by dropping 5 μL of this dispersed solution onto the pretreated GCE with a microsyringe. After air drying for 8 h, the SGNF/GCE was obtained.

AuNPs/GCE was also prepared for comparison. To remove the loose adsorbed substances, the as-prepared GCE was rinsed using distilled water. This was followed by immersing the as-prepared GCE into chloroauric acid solution (25 mM) + sodium sulfate solution (0.1 M) as electrolyte. On the other hand, gold nanoparticles were electrochemically deposited for 300 s at a potential of −0.4 V. Thus, the AuNPs/SGNF-modified GCE was fabricated. The preparation of AuNPs-modified GCE and SNF-modified GCE was comparable to that of the AuNPs/SGNF-modified GCE for a comparative analysis.

3. RESULTS AND DISCUSSION

For the preparation of the AuNPs modified GCE, the electrode was immersed into a chloroauric acid solution (25 mM) + sodium sulfate solution (0.1 M) for 300 s at a potential of −0.4 V. A gold thin film was formed on the GCE surface. The AuNPs-modified electrode in blank PBS solution (0.1 M) was characterized via cyclic voltammogram (CV) profiles, as shown in Fig. 1. Here, a pair of unsymmetrical redox peaks was observed with an anodic peak at 0.695 V, suggesting that Au surface oxides were formed, and a cathodic peak at 0.297 V, indicating that these Au surface oxides were reduced. This phenomenon also demonstrated that AuNPs were successfully deposited on the surface of glass carbon electrode [31].

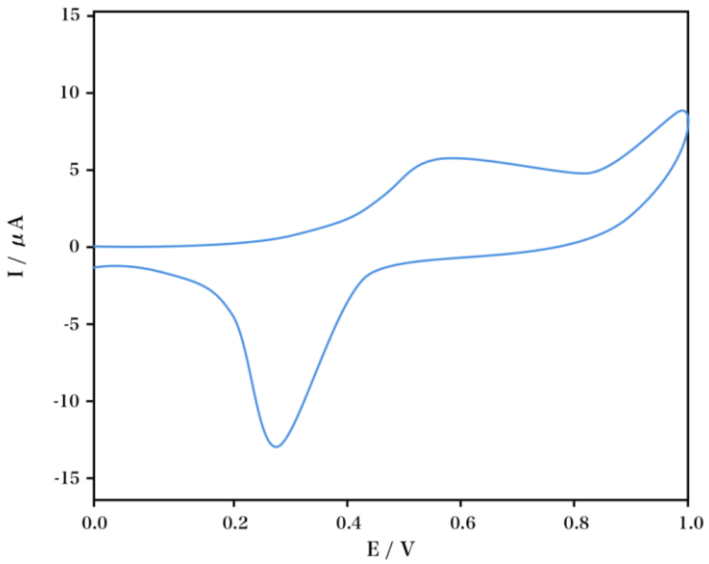

Figure 1. CV profiles of AuNPs modified GCE in blank PBS solution (0.1 M). Scan rate: 100 mV/s.

CV and EIS measurements were performed for the electrochemical features of the bare GCE, AuNPs-modified GCE, SGNF-modified GCE and AuNPs/SGNF-modified GCE. The CV profiles of these GCEs in the $[Fe(CN)_6]^{3-/4-}$ solution (10 mM) + KCl (0.1 M) are displayed in Fig. 2A. It can be seen that the bare GCE exhibited a couple of redox peaks, and a peak-to-peak difference (ΔE_p) of 307 mV was observed. As indicated in curve b, the ΔE_p of the AuNPs-modified GCE was 149 mV, and an increase in the redox peak currents of $[Fe(CN)_6]^{3-/4-}$ was observed, which may be related to the electrocatalytic activity and large specific surface area of AuNPs. After the SGNF modification, a

further ΔE_p decrease and redox peak currents increase were observed, suggesting that the charge transfer was significantly enhanced after the addition of the exceptionally electrically conductive SGNF. After modification of AuNPs/SGNF, a pair of well-defined redox peaks was recorded, (ΔE_p, 115 mV), suggesting that the AuNPs/SGNF-modified GCE exhibited the best electrochemical reversibility among these GCEs. These phenomena may be attributed to the excellent electrocatalytic activity, high conductivity, large specific surface area and synergistic effect of the AuNPs and the SGNF [32, 33].

Electrochemical impedance spectroscopy is a frequency domain measurement method, which can be measured over a wide frequency range. Thus, we can obtain more information about the dynamics and the electrode interface structure than by using the conventional electrochemical methods. A linear segment at a lower frequency and a semicircle segment at a higher frequency constitute a typical Nyquist plot, indicating the electron-transfer resistance (R_{et}), the diffusion limited process, and the electron-transfer resistance (R_{et}), respectively. The bare GCE, AuNPs-modified GCE, SGNF-modified GCE and AuNPs/SGNF-modified GCE were characterized via the EIS profiles as shown in Fig. 2B. The bare GCE showed a R_{et} of 264 Ω, obtained through data fitting with an appropriate equivalent circuit. The R_{et} of the AuNPs-modified GCE was decreased to 201.0 Ω, possibly because the AuNPs possessed large specific surface area and distinct electrocatalytic activity. After modification with SGNF, the electron transfer resistance to the $[Fe(CN)_6]^{3-/4-}$ was further reduced. Furthermore, the SGNF-modified GCE exhibited a R_{et} of 93.07 Ω, which is much lower than that of other GCEs, indicating that the $[Fe(CN)_6]^{3-/4-}$ redox probe - electrode surface charge transfer was enhanced by the highly conductive SGNF. After modification of the AuNPs/SGNF, the lowest R_{et} was recorded. A sharp R_{et} decrease to 1.44 Ω suggested that the charge transfer between the electrode interface and solution was promoted by the AuNPs and SGNF on the electrode surface, considering the exceptional conductivity. Moreover, these results also indicated that SGNF and AuNPs were successfully modified on the GCE surface, and the resulting composite modified electrode showed a higher conductivity activity than the bare GCE, AuNPs/GCE and SGNF/GCE.

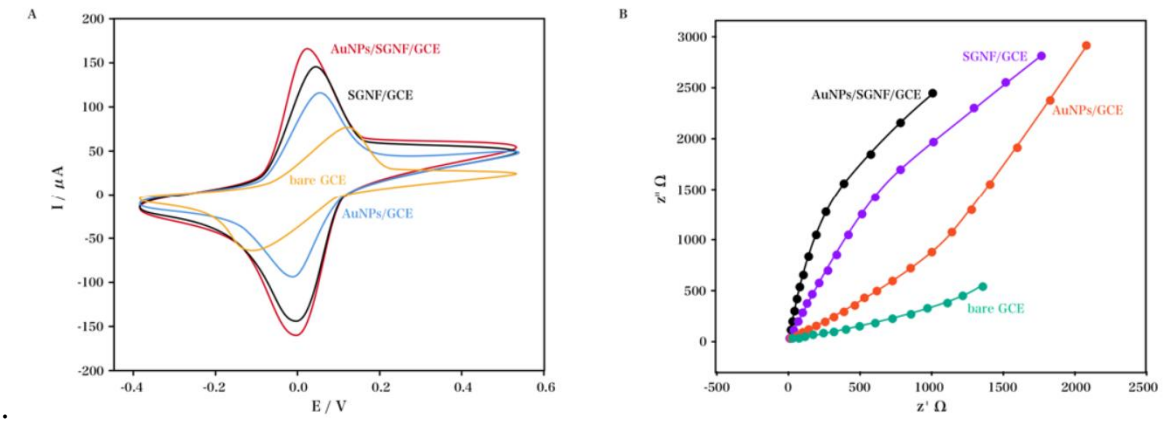

Figure 2. (A) CV profiles and (B) Nyquist plots of bare GCE, AuNPs modified GCE, SGNF modified GCE and AuNPs/SGNF modified GCE in $[Fe(CN)_6]^{3-/4-}$ (10.0 mM) containing KCl (0.1 M). Scan rate for CV: 100 mV/s. Amplitude for EIS was 10 mV.

Fig. 3 shows the DPV profiles of capecitabine (50 μM) obtained using the bare GCE and modified GCEs. In the case of the AuNPs/SGNF-modified GCE, capecitabine exhibited a well-defined reduction peak at −0.768 V. Under comparable conditions, capecitabine showed a reduction potential of −0.844 V when using bare GCE, and those of the AuNPs-modified GCE and SGNF-modified GCE were obtained as −0.802 and −0.769 V, respectively. The reduction potential of capecitabine showed a considerable positive shift, suggesting that the AuNPs/SGNF-modified GCE was catalytic for the reduction of capecitabine. It can be seen that the electron transfer was enhanced by the synergic effects of the appropriate electronic features of AuNPs and SGNF. Among the bare GCE and modified GCEs, the AuNPs/SGNF-modified GCE showed the highest cathodic current for capecitabine reduction. Therefore, the addition of AuNPs and SGNF to the GCE structure led to a factor of 2.9 increase in the voltammetric response. In addition, the reduction peak potential was observed on the less negative side upon doping with the AuNPs and SGNF. Coupled with this effect, the nanocomposite structure formed by the combination of AuNPs and SGNF with an excellent conductivity increased the activity and sensitivity of the newly prepared modified electrode toward capecitabine [34].

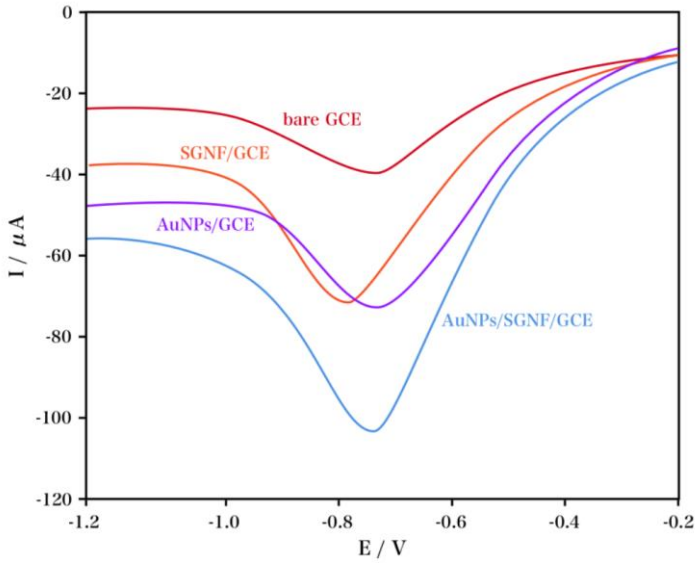

Figure 3. DPV profiles of bare GCE, AuNPs modified GCE, SGNF modified GCE and AuNPs/SGNF modified GCE to the detection of capecitabine (50 μM). Step potential: 2 mV; Pulse amplitude: 25 mV; Scan rate: 10 mV/s; Sampling time: 20 ms; Pulse interval: 100 ms.

To study the influence of pH on the peak current (I) and the reduction peak potential (E_{pc}) of capecitabine (50.0 μM), we performed DPV measurements. The voltammetric response of capecitabine using the AuNPs/SGNF-modified GCE was investigated at different pH values, including pH 2.0, 2.5, 3.0, 4.0 and 5.0. Fig. 4 shows the effect of pH on the peak current. A gradual decrease in the reduction peak current was observed with increasing pH in the 2.0-5.0 range. Therefore, pH 2.0 PBS was used as the electrolyte for the subsequent measurements. The effect of pH on the peak potential was also investigated. As the pH was increased in the 2.0 - 5.0 range, the reduction potential

of capecitabine was positively shifted using the AuNPs/SGNF-modified GCE. This confirms that protons participate in the electrochemical reactions.

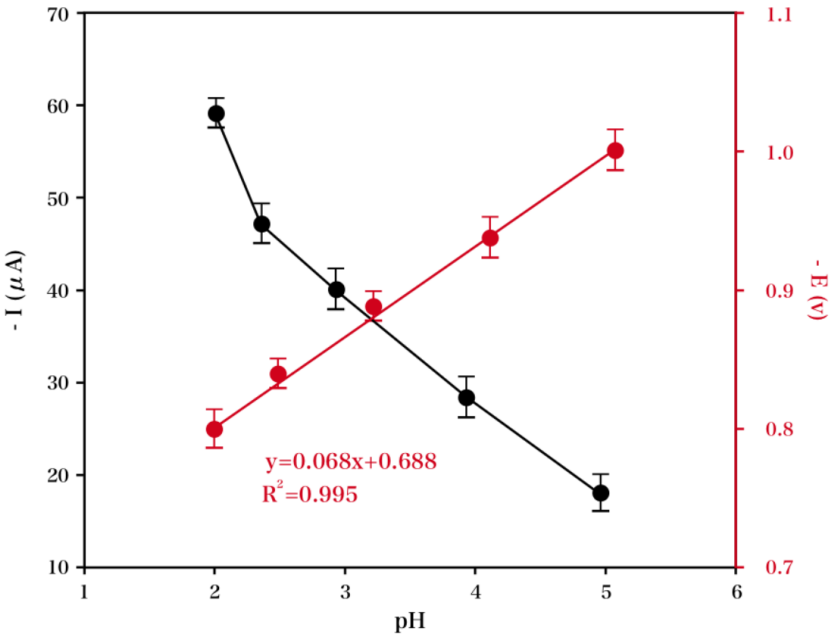

Figure 4. Effect of pH on the cathodic peak current and cathodic peak potential.

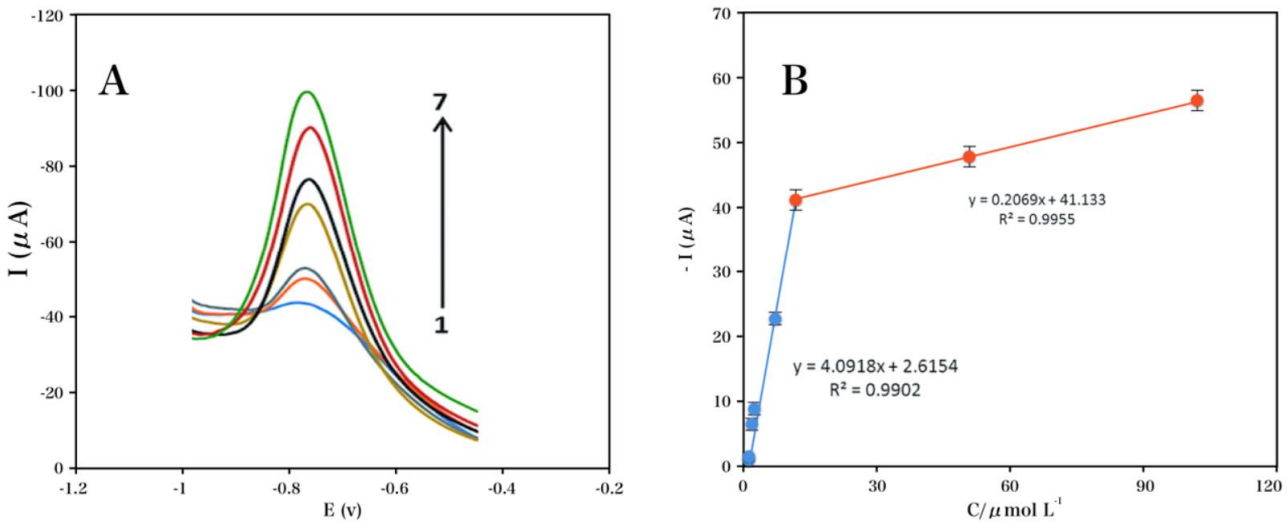

Figure 5. (A) DPV profiles for capecitabine (0.05, 0.1, 2.0, 5.0, 10.0 (5), 40.0, and 80.0 μM) using AuNPs/SGNF modified GCE in PBS. (B) Plots of the peak current as a function of capecitabine concentration (0.05–80.0 μM). Step potential: 2 mV; Pulse amplitude: 25 mV; Scan rate: 10 mV/s; Sampling time: 20 ms; Pulse interval: 100 ms.

The parameters of the capecitabine detection using the AuNPs/SGNF-modified GCE were optimized. The DPVs of varying concentrations of capecitabine are shown in Fig. 5A. Each DPV

profile exhibited an obvious reduction peak. As the concentration increased in the 0.05-80.0 μM range, a current increase was recorded. Fig. 5B shows the dependence of peak current on capecitabine concentration, where the peak current was proportional to its corresponding concentration with the LOD of 0.017 μM (measured under $3S_b/m$). For comparison to previous reports, the characteristics of different electrochemical sensors for capecitabine are summarized in Table 1.

Table 1. Comparison of the major characteristics of electrochemical sensors used for the detection of capecitabine.

Electrode	Linear detection range	Detection limit	Reference
HPLC+ultraviolet detection	—	0.01 mg/mL	[35]
CPE	300-3000.0 μM	82.3 μM	[36]
ZnO/MWCNT/CPE	0.1-100.0 μM	0.03 μM	[18]
AuNPs/SGNF/GCE	0.05-80.0 μM	0.017 μM	This work

We also studied the reproducibility of the AuNPs/SGNF-modified GCE for the detection of capecitabine. For six consecutive experiments using varying capecitabine concentrations, the reduction current showed a standard deviation of approximately 2.74%. To study stability, the AuNPs/SGNF-modified GCE was stored at ambient temperature in air. Overall, 96.6% of the initial activity of this GCE remained after over 15 days. Thus, it can be seen that the AuNPs/SGNF-modified GCE was highly stable and the obtained results were reproducible.

The practical application of our developed sensor towards the determination of capecitabine concentration in real serum specimens was also investigated. For the recovery test, the standard capecitabine solution was spiked into the diluted real specimens. For the spiked serum specimen, the capecitabine recovery ranged from 101.48 to 105.21%, suggesting the suitability of our proposed strategy for the determination of capecitabine concentration in triplicate analysis, with the corresponding results shown in Table 2.

Table 2. Detection of capecitabine in serum specimen with our developed AuNPs/SGNF modified GCE.

Sample	Added (μM)	Found (μM)	Recovery (%)	RSD (%)
1	—	None	—	2.65
2	5	5.074	101.48	3.30
3	10	10.521	105.21	2.78

4. CONCLUSIONS

This work described the fabrication of a novel electrochemical sensor based on the AuNPs/SGNF-modified GCE for a sensitive detection of trace-level capecitabine. Our proposed sensor showed quantitatively reproducible results, high long-term stability, and exceptional electrocatalytic

activity for capecitabine oxidation, thus demonstrating its potential for the detection of capecitabine in real specimens as an electrochemical sensor. Using DPV measurements, the calibration curve was in the linear range of 0.05–80.00 μM of capecitabine concentration, and the LOD was calculated as 0.0171 μM.

References

1. C.E. Geyer, J. Forster, D. Lindquist, S. Chan, C.G. Romieu, T. Pienkowski, A. Jagiello-Gruszfeld, J. Crown, A. Chan and B. Kaufman, *New England Journal of Medicine*, 355 (2006) 2733.
2. K.D. Miller, L.I. Chap, F.A. Holmes, M.A. Cobleigh, P.K. Marcom, L. Fehrenbacher, M. Dickler, B.A. Overmoyer, J.D. Reimann and A.P. Sing, *Journal of clinical oncology*, 23 (2005) 792.
3. J.L. Blum, S.E. Jones, A.U. Buzdar, P.M. LoRusso, I. Kuter, C. Vogel, B. Osterwalder, H.-U. Burger, C.S. Brown and T. Griffin, *Journal of Clinical Oncology*, 17 (1999) 485.
4. I.E. Krop, N.U. Lin, K. Blackwell, E. Guardino, J. Huober, M. Lu, D. Miles, M. Samant, M. Welslau and V. Diéras, *Annals of Oncology*, 26 (2015) 113.
5. T. Bachelot, G. Romieu, M. Campone, V. Diéras, C. Cropet, F. Dalenc, M. Jimenez, E. Le Rhun, J.-Y. Pierga and A. Gonçalves, *The lancet oncology*, 14 (2013) 64.
6. P.A. Kaufman, A. Awada, C. Twelves, L. Yelle, E.A. Perez, G. Velikova, M.S. Olivo, Y. He, C.E. Dutcus and J. Cortes, *Journal of clinical oncology*, 33 (2015) 594.
7. M. Welslau, V. Diéras, J.H. Sohn, S.A. Hurvitz, D. Lalla, L. Fang, B. Althaus, E. Guardino and D. Miles, *Cancer*, 120 (2014) 642.
8. J. Gligorov, D. Doval, J. Bines, E. Alba, P. Cortes, J.-Y. Pierga, V. Gupta, R. Costa, S. Srock and S. de Ducla, *The Lancet Oncology*, 15 (2014) 1351.
9. H. Joensuu, P.-L. Kellokumpu-Lehtinen, R. Huovinen, A. Jukkola-Vuorinen, M. Tanner, R. Kokko, J. Ahlgren, P. Auvinen, O. Saarni and L. Helle, *Acta Oncologica*, 53 (2014) 186.
10. M.M. Mita, A.A. Joy, A. Mita, K. Sankhala, Y.-M. Jou, D. Zhang, P. Statkevich, Y. Zhu, S.-L. Yao and K. Small, *Clinical breast cancer*, 14 (2014) 169.
11. C. Saura, J.A. Garcia-Saenz, B. Xu, W. Harb, R. Moroose, T. Pluard, J. Cortés, C. Kiger, C. Germa and K. Wang, *Journal of Clinical Oncology*, 32 (2014) 3626.
12. G. Curigliano, V. Bagnardi, F. Bertolini, M. Alcalay, M.A. Locatelli, L. Fumagalli, C. Rabascio, A. Calleri, L. Adamoli and C. Criscitiello, *The Breast*, 24 (2015) 263.
13. E. Montagna, A. Palazzo, P. Maisonneuve, G. Cancello, M. Iorfida, A. Sciandivasci, A. Esposito, A. Cardillo, M. Mazza and E. Munzone, *Cancer Letters*, 400 (2017) 276.
14. A. Morikawa, D.M. Peereboom, H.R. Thorsheim, R. Samala, R. Balyan, C.G. Murphy, P.R. Lockman, A. Simmons, R.J. Weil and V. Tabar, *Neuro-oncology*, 17 (2014) 289.
15. J.A. O'Shaughnessy, H. Koeppen, Y. Xiao, M.R. Lackner, D. Paul, C. Stokoe, J. Pippen, L. Krekow, F. Holmes and S. Vukelja, *Clinical Cancer Research*, (2015) clincanres.
16. C.H. Smorenburg, S.M. De Groot, A.E. van Leeuwen-Stok, M.E. Hamaker, A.N. Wymenga, H. de Graaf, F.E. de Jongh, J.J. Braun, M. Los and E. Maartense, *Annals of oncology*, 25 (2014) 599.
17. M. Martin, J. Bonneterre, C.E. Geyer, Y. Ito, J. Ro, I. Lang, S.-B. Kim, C. Germa, J. Vermette and K. Wang, *European journal of cancer*, 49 (2013) 3763.
18. T. Madrakian, H. Ghasemi, E. Haghshenas and A. Afkhami, *RSC Advances*, 6 (2016) 33851.
19. P. Deng, C. Ji, X. Dai, D. Zhong, L. Ding and X. Chen, *Journal of Chromatography B*, 989 (2015) 71.
20. E. Piórkowska, M. Kaza, J. Fitatiuk, I. Szlaska, T. Pawiński and P.J. Rudzki, *Die Pharmazie-An International Journal of Pharmaceutical Sciences*, 69 (2014) 500.
21. M.J. Deenen, H. Rosing, M.J. Hillebrand, J.H.M. Schellens and J.H. Beijnen, *Journal of Chromatography B*, 913 (2013) 30.

22. S. Hassanlou, M. Rajabi and M. Afshar, *South African Journal of Chemistry*, 69 (2016) 174.
23. A. Ambrosi and M. Pumera, *Physical Chemistry Chemical Physics*, 12 (2010) 8943.
24. C.L. Scott, G. Zhao and M. Pumera, *Electrochemistry Communications*, 12 (2010) 1788.
25. X. Niu, W. Yang, H. Guo, J. Ren, F. Yang and J. Gao, *Talanta*, 99 (2012) 984.
26. C.L. Scott and M. Pumera, *Electroanalysis*, 23 (2011) 858.
27. C. Wang, J. Du, H. Wang, C.e. Zou, F. Jiang, P. Yang and Y. Du, *Sensors and Actuators B: Chemical*, 204 (2014) 302.
28. Y. Zhang, G.M. Zeng, L. Tang, J. Chen, Y. Zhu, X.X. He and Y. He, *Analytical chemistry*, 87 (2015) 989.
29. F. Arduini, C. Zanardi, S. Cinti, F. Terzi, D. Moscone, G. Palleschi and R. Seeber, *Sensors and Actuators B: Chemical*, 212 (2015) 536.
30. J. Ji, Z. Zhou, X. Zhao, J. Sun and X. Sun, *Biosensors and Bioelectronics*, 66 (2015) 590.
31. P. Khashayar, G. Amoabediny, M. Hosseini, R. Verplancke, F. Razi, J. Vanfleteren and B. Larijani, *IEEE Sensors Journal*, 17 (2017) 3367.
32. D. Zhu, Q. Li, X. Pang, Y. Yuan and G. Chen, *Food Analytical Methods*, 9 (2016) 1963.
33. M. Patricia Khashayar and P.R.V. Morteza Hosseini, *Sensors*, 17069 (2017) 1.
34. C.T.P. da Silva, F.R. Veregue, L.W. Aguiar, J.G. Meneguin, M.P. Moisés, S.L. Fávaro, E. Radovanovic, E.M. Girotto and A.W. Rinaldi, *New Journal of Chemistry*, 40 (2016) 8872.
35. L. Zufía, A. Aldaz and J. Giráldez, *Journal of Chromatography B*, 809 (2004) 51.
36. X. LIN, Y. ZHANG, L. LI, T. ZHAN and N. HUI, *Journal of Qingdao Agricultural University (Natural Science)*, 3 (2012) 015.